Tunable beam deflection based on plasmonic resonators mounted freestanding thermoresponsive hydrogel

Ata Ur Rahman Khalid, Juan Liu (刘 娟)*, Naeem Ullah, and Shiqi Jia (贾世琪)

Beijing Engineering Research Center for Mixed Reality and Advanced Display, School of Optics and Photonics, Beijing Institute of Technology, Beijing 100081, China

**Corresponding author: juanliu@bit.edu.cn*

Received January 8, 2020; accepted March 6, 2020; posted online May 13, 2020

We propose and numerically demonstrate a dynamic beam deflector based on plasmonic resonator loaded thermoresponsive freestanding hydrogel that swells and collapses in water by temperature. For this purpose, we utilize four-step phase gradients mounted on freestanding hydrated hydrogel. For normal incidence, linearly orthogonal light deflects to 19.44° in the collapsed state and 14.40° in the swollen state of hydrogel. Furthermore, the light deflects at a third angle of 12.29° when the solvent changes from water to ethanol. It is expected that our metadesign will provide a platform for dynamic holography, active lensing, data storage, and anticounterfeiting.

Keywords: tuning; beam deflector; hydrogel.
doi: 10.3788/COL202018.062402.

Metasurfaces, artificially engineered structures, have received tremendous attention because of their unique feature to control electromagnetic (EM) waves. The geometric control of structures results in fascinating phenomena that barely exist in nature such as negative refraction, cloaking, the Doppler effect, and optical focusing[1–5]. By taking control over the propagation of EM waves, metasurfaces are widely being studied in flat lensing, vortex beam generation, and holograms[6–11].

Metasurfaces can produce various profiles for outgoing electromagnetic waves. Thus, arbitrary wavefronts can be obtained by simply arranging the meta-atoms. A beam deflector is an important optical component used in steering the light in a specific direction[12]. Nanostructures are playing a vital role in manipulating outgoing wavefronts and providing new avenues to develop various nano-optics devices. Till now, several approaches have been reported for beam steering by using subwavelength structures such as gratings[13], metallic slits[14], slits filled with nonlinear materials[15], and plasmonic and dielectric metasurfaces[12,16,17]. However, active steering of light by using metasurfaces is highly desired in practical applications. Among the studies concerning active steering there is some research to actively control the light path by temperature stimulation[18–22], external strain[23], and electrical gating[24,25]. The studies based on phase change material either use separate types of meta-atom that are dominantly reactive or less reactive based on temperature variation degrading the signal to noise ratio, or use complex structures that are difficult to fabricate. Furthermore, an electrical gating restricts the deflection angle range, and external strain structures might not be quite feasible to integrate with practical applications. Here, we are the first time to use functional hydrogel that swells and collapses by temperature stimulation in water instead of external strain.

Hydrogel, poly(N-isopropylacrylamide-based) (pNIPAAM) membrane, extensively swells and collapses vertically (surface-attached hydrogel) or horizontally (freestanding hydrogel) inside water by temperature stimulation. In an aqueous solution, such a hydrophilic polymeric network absorbs a considerable amount of water and attains the equilibrium swelling state below the local critical solution temperature (LCST). The increase of temperature from the LCST oozes the water and results in the collapse of the polymeric network[26,27]. The swelling and collapse occur with a characteristic response time below 100 ms and are fully reversible up to several hundreds of cycles[28]. Previously, it has been studied for actively tunable collective surface plasmons[29], active control of surface plasmon resonance for biosensor applications[28], and dynamic holography[30]. Due to the swelling and collapsing feature, metasurface integrated hydrogel has great potential to manipulate wavefronts. The phase discontinuity can be tuned by changing the scattering element, shape, orientation, and position of each element. Among these tuning mechanisms, the relative position of meta-atoms can be changed by using resonator loaded freestanding hydrogel. The freestanding hydrogel swells and collapses in water and provides additional swelling in ethanol. The swelling in ethanol is not reversible by temperature. However, changing the solvent to water, the hydrogel regains its reversible switching[29]. Here, we demonstrate that by mounting the resonators on freestanding hydrogel, the outgoing wavefront can be tuned at three different angles via temperature modulation and solvent. We believe that our approach can find applications in active photonic fields such as fiber-optics telecommunication, scanning systems, and integrated optical devices.

Figure 1 illustrates the schematic of the proposed tunable beam deflector. We periodically arrange the resonators on freestanding hydrogel, which swells and collapses

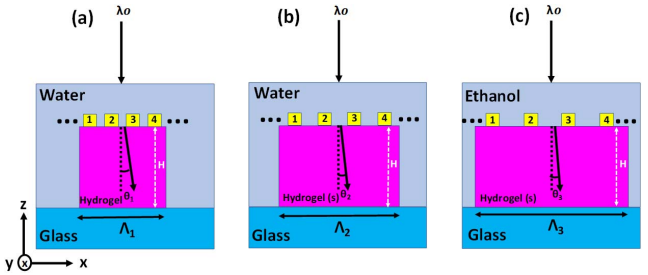

Fig. 1. Schematic of the tunable beam deflector. The array of resonators is loaded on the surface of hydrogel. (a) Hydrogel in water after the T_{LCST}, (b) hydrogel in water before the T_{LCST}, (c) hydrogel in ethanol. The letter "s" in parentheses stands for swollen hydrogel. Periodic arrays of optimized resonators are loaded on hydrogel from which the set of four resonators makes a supercell. The sizes of supercells in the x direction in each condition are denoted by Λ_1, Λ_2, and Λ_3, respectively. θ_1, θ_2, and θ_3 are the corresponding deflection angles in each condition, respectively. Also, $\Lambda_3 > \Lambda_2 > \Lambda_1$. H is the height of the hydrogel.

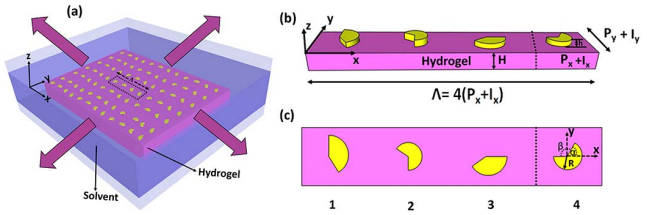

Fig. 2. Design of the meta-atoms on the freestanding hydrogel dipped in solvent. (a) The meta-atoms consist of gold sector resonators patterned on the surface of the freestanding hydrogel. The arrows indicate the swelling in solvent in the x and y directions. (b) The supercell. H and h are the height of the hydrogel and sector resonator, respectively. $P_x = P_y$ is the periodicity of the unit cell. I_x and I_y are the increment of the period in the x and y directions, respectively. Λ is the total size of the supercell in the x direction. The rightmost cell depicts the basic building block. (c) The top view of the optimized four resonators. The α and β are the opening angles, and R is the radius of the sector resonator.

in water by temperature. Due to the swelling and collapsing of hydrogel, the linearly orthogonal transmitted light deflects between θ_1 and θ_2 by temperature modulation [Figs. 1(a) and 1(b)]. The outgoing light further deflects at θ_3 due to further swelling in ethanol [Fig. 1(c)]. The light deflection follows the generalized Snell's law[31]:

$$n_t \sin\theta_t - n_i \sin\theta_i = \frac{\lambda_o}{2\pi}\frac{\mathrm{d}\Phi}{\mathrm{d}x}, \tag{1}$$

where n_i and n_t are the indices of refraction in the incidence and refraction medium, respectively. θ_i and θ_t are the incidence and refraction angles, respectively, λ_o in the freespace wavelength, $\mathrm{d}\Phi$ is the phase difference between the successive unit cells, and $\mathrm{d}x$ is the period of a unit cell. For the normal incidence $\theta_i = 0$ with hydrogel as the refraction medium, the anomalous refraction angle can be obtained by $|\theta_t| = \arcsin(\lambda_o/n_t\Lambda)$, where Λ is the size of the supercell in the x direction. The refraction angle $|\theta_t|$ can be tuned by Λ, which is in an inverse proportional relationship with Λ. Thus, the refraction angle decreases with the increase in size of the supercell and vice versa.

Our metadesign consists of periodically arranged resonators sitting on the top surface of freestanding hydrogel dipped in a solvent inside the glass container, as depicted in Fig. 2(a). The dotted rectangle is representing a supercell with period of Λ in the x direction. Figures 2(b) and 2(c) represent the supercell and its top view, respectively. The building block of the metasurface consists of circular sectors/segments on the top of the thermoresponsive hydrogel, as shown in the rightmost cell of Fig. 2(b). The 2D illustration of the unit cell is presented in Fig. 2(c), the rightmost cell. The antennas on the top of the hydrogel are called sector resonators throughout this Letter. By varying the first opening of sector α (angle w.r.t. the x axis in the conterclockwise direction), the second opening of sector resonator β (angle w.r.t. α in the counterclockwise direction), and radius R, the amplitude and phase of scattered light can locally be modulated. In this study, we choose freestanding hydrogel that swells and collapses in lateral directions in water. When it interacts with water below LCST, i.e., 32°C, then it swells and collapses back after the LCST. The hydrogel further expands when it interacts with ethanol. It exhibits a nonthermoresponsive property in ethanol. We take the refractive index of freestanding hydrogel in water as follows: in a swollen state $n_s = 1.34$ and in a collapsed state $n_c = 1.46$, while the surrounding water has a refractive index $n_w = 1.334$. In ethanol, the refractive index in the swelling state $n_s = 1.37$, while the surrounding ethanol refractive index $n_e = 1.36$. These indices are taken from Ref. [29]. The operating wavelength is 700 nm.

We carry out numerical simulations to optimize the parameters by the finite difference time domain (FDTD) method by the commercially available simulation tool from Lumerical FDTD solutions. We conduct a parametric sweep by changing α, β, and R, while the hydrogel height $H = 4\,\mu\mathrm{m}$ and the sector resonator height $h = 35\,\mathrm{nm}$ to obtain complete $0-2\pi$ phase coverage of uniform amplitude when the sector resonator loaded hydrogel is dipped in water and the solution temperature is $T > T_{\mathrm{LCST}}$, i.e., the collapsed state. Initially, we set the period $P_x = P_y = 360\,\mathrm{nm}$; therefore $I_x = I_y = 0$ in the collapsed state. The incident light is linearly y polarized normal to the resonator from the $+z$ axis. The periodic boundary conditions are used in both the x and y directions while the perfect matched layers condition is applied in the z direction. The linearly x-polarized light is collected in transmission for analysis. We delicately select two resonators to achieve a π phase shift with a uniform amplitude modulation. A complete phase coverage of $0-2\pi$ can be realized by rotating the selected resonators by 90° [Fig. 3 (red line)]. The opening angles and the corresponding radii of four resonators are listed in Table 1. By decreasing the temperature below the T_{LCST} the hydrogel swells and the period increases from $P_x = P_y = 360\,\mathrm{nm}$

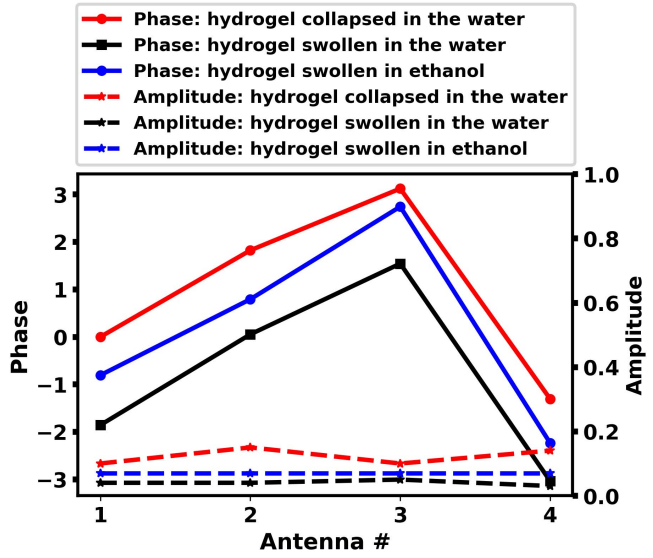

Fig. 3. The phases (red, black, and blue lines) and amplitude values (red, black, and blue starred dash lines) of the optimized resonators in the swollen and collapsed states of hydrogel.

Table 1. Parametric Values of Optimized Four Sector Resonators[a]

	Antennas			
Parameters	1	2	3	4
α	90°	150°	0°	60°
β	210°	120°	210°	120°
R (nm)	150	110	150	110

[a]The height h is constant at 35 nm.

to $P_x = P_y = 525\,\text{nm}$, and therefore $I_x = I_y = 165\,\text{nm}$. Consequently, each antenna receives additional phase equally, and thus the relative phase covers the complete 2π phase span [Fig. 3 (black line)]. The same effect appears when we dip the hydrogel in the ethanol solution, as illustrated in Fig. 3 (blue line). In all these three conditions we get an almost uniform amplitude, as depicted in Fig. 3 (red, black, and blue dashed lines, respectively).

To demonstrate the proposed tunable beam deflector, we introduce phase gradients on the surface of hydrogel. We arrange selected four phase gradients $\mathrm{d}\Phi/\mathrm{d}x$ on freestanding hydrogel such that corresponding phases gradually cover a 2π phase distribution with a step of $\pi/2$ [Figs. 2(b) and 2(c)], which forms the supercell. This arrangement causes incoming light to deflect in a specific direction according to the generalized Snell's law as calculated by

$$\theta_1 = |\theta_t| = \arcsin\left(\frac{\lambda_o}{n_t\Lambda_1}\right) = \arcsin\left(\frac{700\,\text{nm}}{1.46 \times 1440\,\text{nm}}\right) = 19.44°, \quad (2)$$

$$\theta_2 = |\theta_t| = \arcsin\left(\frac{\lambda_o}{n_t\Lambda_2}\right) = \arcsin\left(\frac{700\,\text{nm}}{1.34 \times 2100\,\text{nm}}\right) = 14.40°, \quad (3)$$

$$\theta_3 = |\theta_t| = \arcsin\left(\frac{\lambda_o}{n_t\Lambda_3}\right) = \arcsin\left(\frac{700\,\text{nm}}{1.37 \times 2400\,\text{nm}}\right) = 12.29°. \quad (4)$$

Equations (2)–(4) depict the analytical computed angles for hydrogels collapsed in water, swollen in water, and swollen in ethanol, respectively. When the hydrated hydrogel is in a collapsed state, i.e., $I_x = I_y = 0$, then the size of the supercell in the x direction becomes $\Lambda = \Lambda_1 = 4 \times (P_x + I_x) = 1440\,\text{nm}$. For normal incidence, outgoing light deflects at an angle of $\theta_1 = 19.44°$ in hydrogel. When the solvent temperature is less than the critical solution temperature, the hydrogel swells in both the x and y directions, and thus the size of the supercell in the x direction becomes $\Lambda = \Lambda_2 = 4 \times (P_x + I_x) = 2100\,\text{nm}$, where $I_x = I_y = 165\,\text{nm}$. Thus, under swelling conditions, the light deflects at $\theta_2 = 14.40°$. The light further deflects to $\theta_3 = 12.29°$ by changing the solvent from water to ethanol. This is due to the fact that ethanol serves as a better solvent than water. In ethanol, the period of the unit cell prolonged with the increment of $P_x = P_y = 240$ nm in both the x and y directions. Thus, the size of the supercell in the x direction becomes $\Lambda = \Lambda_3 = 4 \times (P_x + I_x) = 2400$ nm in ethanol. These analytically computed angles are in accordance with simulated ones at the linearly orthogonal outgoing light when the linearly y polarized light impinges, and the sector loaded hydrogel is dipped in different solvents and stimulated with temperature. Figures 4(a)–4(c) show the phase distribution inside the hydrogel for the outgoing light under swelling and collapsing in water and swelling in ethanol, respectively. The light further deflects at 19.52°, 13.24°, and 11.56° under swelling and collapsing in water and swelling in ethanol, respectively, inside the glass due to mismatch of refractive indices of hydrogel and glass, as shown in Figs. 4(d)–4(f).

The angle deflection in water is dynamic, which exhibits deflection angle switching due to the swelling and collapsing of hydrogel through temperature modulation. In ethanol, hydrogel does not exhibit active deflection by changing the temperature. However, by changing the solvent to water, hydrogel again functions actively by temperature modulation. In the case of reversing the incident polarization to x polarized light, the phase gradients must have to be arranged along the y axis to observe the linearly orthogonal beam deflection. The overall absorption of our water-dipped plasmonic metadesign is high, and thus only a limited amount of energy will be transmitted, i.e., 2%. Furthermore, our proposed design can be fabricated by using the approach reported in Ref. [29]. The fabrication steps are as follows: pattern the sector resonator supercell arrays on glass substrate via state of the art electron beam lithography technique, then attach the pNIPAAM layer by *in situ* synthesizing via UV light irradiation, and

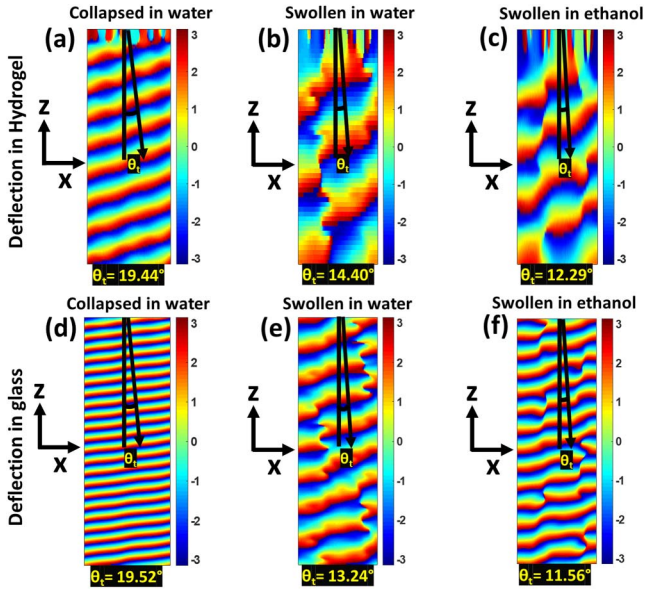

Fig. 4. Numerical simulation results. (a)–(c) are the phase distributions of the wavefront inside the hydrogel in a collapsed state in water, swollen in water, and swollen in ethanol, respectively. (d)–(f) are the phase distributions of the wavefront inside the glass in a collapsed state in water, swollen in water, and swollen in ethanol, respectively. θ_t is the refraction angle in the xy plane for the linearly y-polarized input light and the linearly x-polarized light is calculated at output.

detach the patterned hydrogel from the glass substrate by swelling in ethanol in order to form a freestanding membrane.

In conclusion, we have numerically demonstrated the dynamic deflection of the wavefront by using plasmonic resonator loaded freestanding thermoresponsive hydrogel. By arranging the sector resonators on hydrogel, we observe anomalous refraction. When the solution temperature is greater than the LCST, i.e., collapsed state, the outgoing linearly orthogonal light deflects at 19.46° in hydrated hydrogel from the normal. Similarly, the deflection angle tunes from 19.46° to 14.40° due to the increase in period when the hydrated hydrogel is in the swollen state. This tunability is reversible in water via temperature modulation. Furthermore, the outgoing light further deflects to 12.29° due to better swelling in ethanol. The deflection in ethanol is not reversible by temperature. However, the hydrogel will function actively again when the solvent changes back to water. It is predicted that such active meta devices may serve as a novel platform for active switching, active lensing, anticounterfeiting, and several other flat optical devices in optical fiber-optics communication and scanning systems that demand highly compact light path deflection and fast switching.

This work was supported by the National Key R&D Program of China (No. 2017YFB1002900), the National Natural Science Foundation of China (NSFC) (Nos. 61575024, 61420106014, and 61975014), and the United Kingdom Government's Newton Fund.

References

1. S. H. Lee, C. M. Park, Y. M. Seo, and C. K. Kim, Phys. Rev. B **81**, 241102 (2010).
2. J. Ran, Y. Zhang, X. Chen, K. Fang, J. Zhao, Y. Sun, and H. Chen, Sci. Rep. **5**, 11659 (2015).
3. R. A. Shelby, D. R. Smith, and S. Schultz, Science **292**, 77 (2001).
4. J. Valentine, J. Li, T. Zentgraf, G. Bartal, and X. Zhang, Nat. Mater. **8**, 568 (2009).
5. D. Ye, K. Chang, L. Ran, and H. Xin, Nat. Commun. **5**, 5851 (2014).
6. K. E. Chong, I. Staude, A. James, J. Dominguez, S. Liu, S. Campione, G. S. Subramania, T. S. Luk, M. Decker, D. N. Neshev, I. Brener, and Y. S. Kivshar, Nano Lett. **15**, 5369 (2015).
7. Q. Jiang, G. Jin, and L. Cao, Adv. Opt. Photonics **11**, 518 (2019).
8. M. Khorasaninejad, A. Y. Zhu, C. Roques-Carmes, W. T. Chen, J. Oh, I. Mishra, R. C. Devlin, and F. Capasso, Nano Lett. **16**, 7229 (2016).
9. G. Y. Lee, J. Sung, and B. Lee, Comput. Sci. **41**, 10 (2019).
10. M. I. Shalaev, J. Sun, A. Tsukernik, A. Pandey, K. Nikolskiy, and N. M. Litchinitser, Nano Lett. **15**, 6261 (2015).
11. A. U. R. Khalid, J. Liu, Y. Han, N. Ullah, R. Zhao, and Y. Wang, Opt. Commun. **451**, 211 (2019).
12. Q. Zhang, M. Li, T. Liao, and X. Cui, Opt. Commun. **411**, 93 (2018).
13. D. de Ceglia, M. A. Vincenti, and M. Scalora, Opt. Lett. **37**, 271 (2012).
14. T. Xu, C. Wang, C. Du, and X. Luo, Opt. Express **16**, 4753 (2008).
15. M. A. Vincenti, A. D'Orazio, M. Buncick, N. Akozbek, M. J. Bloemer, and M. Scalora, J. Opt. Soc. Am. B **26**, 301 (2009).
16. S. Kita, K. Takata, M. Ono, K. Nozaki, E. Kuramochi, K. Takeda, and M. Notomi, APL Photonics **2**, 046104 (2017).
17. A. A. Rifat, M. Rahmani, L. Xu, K. Z. Kamali, A. Komar, J. Yan, D. Neshev, and A. E. Miroshnichenko, in *Frontiers in Optics* (2018), paper JTu3A.12.
18. T. Cao, G. Zheng, S. Wang, and C. Wei, Opt. Express **23**, 18029 (2015).
19. C. Choi, S. Y. Lee, S. E. Mun, G. Y. Lee, J. Sung, H. Yun, J. H. Yang, H. O. Kim, C. Y. Hwang, and B. Lee, Adv. Opt. Mater. **7**, 1900171 (2019).
20. C. Choi, J. Sung, J.-G. Yun, S.-Y. Lee, S.-J. Kim, and B. Lee, Chin. Opt. Lett. **16**, 050009 (2018).
21. X. Yin, T. Steinle, L. Huang, T. Taubner, M. Wuttig, T. Zentgraf, and H. Giessen, Light Sci. Appl. **6**, e17016 (2017).
22. C. Choi, S.-J. Kim, and B. Lee, in *Conference on Lasers and Electro-Optics/Pacific Rim* (2017), paper s2377.
23. H.-S. Ee and R. Agarwal, Nano Lett. **16**, 2818 (2016).
24. A. L. Holsteen, A. F. Cihan, and M. L. Brongersma, Science **365**, 257 (2019).
25. A. Komar, R. Paniagua-Dominguez, A. Miroshnichenko, Y. F. Yu, Y. S. Kivshar, A. I. Kuznetsov, and D. Neshev, ACS Photonics **5**, 1742 (2018).
26. K. Matsumoto, N. Sakikawa, and T. Miyata, Nat. Commun. **9**, 1 (2018).
27. J. M. Rosiak and F. Yoshii, Nucl. Instrum. Methods Phys. Res. Sect. B **151**, 56 (1999).
28. M. Toma, U. Jonas, A. Mateescu, W. Knoll, and J. Dostalek, J. Phys. Chem. C **117**, 11705 (2013).
29. N. Gisbert Quilis, M. van Dongen, P. Venugopalan, D. Kotlarek, C. Petri, A. Moreno Cencerrado, S. Stanescu, J. L. Toca Herrera, U. Jonas, M. Möller, A. Mourran, and J. Dostalek, Adv. Opt. Mater. **7**, 1900342 (2019).
30. A. U. R. Khalid, J. Liu, Y. Han, N. Ullah, S. Jia, and Y. Wang, Opt. Lett. **45**, 479 (2020).
31. N. Yu, P. Genevet, M. A. Kats, F. Aieta, J. P. Tetienne, F. Capasso, and Z. Gaburro, Science **334**, 333 (2011).